stichting
mathematisch
centrum

MC

AFDELING NUMERIEKE WISKUNDE
(DEPARTMENT OF NUMERICAL MATHEMATICS)

NW 111/81 AUGUSTUS

H. SCHIPPERS

APPLICATION OF MULTIGRID METHODS FOR INTEGRAL EQUATIONS TO TWO PROBLEMS FROM FLUID DYNAMICS

Preprint

kruislaan 413 1098 SJ amsterdam

Printed at the Mathematical Centre, 413 Kruislaan, Amsterdam.

The Mathematical Centre, founded the 11-th of February 1946, is a non-profit institution aiming at the promotion of pure mathematics and its applications. It is sponsored by the Netherlands Government through the Netherlands Organization for the Advancement of Pure Research (Z.W.O.).

1980 Mathematics subject classification: 65N20, 65R20, 76B05, 76U05

Application of multigrid methods for integral equations to two problems from fluid dynamics*)

by

H. Schippers

ABSTRACT

In the present paper multigrid methods are applied in order to solve efficiently the non-sparse systems of equations that occur in the numerical solution of the following problems from fluid dynamics: (1) calculation of potential flow around bodies and (2) calculation of oscillating disk flow. Problem (1) is reformulated as a boundary integral equation of the second kind that is approximated by a first order panel method resulting in a full system of equations. This method is in widespread use for aerodynamic computations. The second problem is described by the Navier-Stokes and continuity equations. By means of the von Kármán similarity transformations these equations are reduced to a nonlinear system of parabolic equations which are approximated by implicit finite difference techniques. From the periodic conditions in time one obtains a non-sparse system of equations. For these two problems from fluid dynamics the fast convergence of multigrid methods for integral equations is established by numerical experiments.

KEY WORDS & PHRASES: *Multigrid methods, potential flow around bodies, oscillating disk flow, Fredholm integral equation of the second kind*

---

*) This report will be submitted for publication elsewhere.

INTRODUCTION

Multigrid methods have been advocated by Brandt (ref.1) for solving sparse systems of equations that arise from discretization of partial differential equations. Convergence and computational complexity of such multigrid techniques have been studied since. In reference 2 we have shown that these techniques can also be used advantageously for the non-sparse systems that occur in the numerical solution of Fredholm integral equations of the second kind

$$f = Kf + g, \tag{1}$$

where g belongs to a Banach space X and the integral operator K is compact on X. Theoretical and numerical investigations show that multigrid methods give the solution of (1) in $O(N^2)$ operations as $N \to \infty$, whereas other iterative schemes take $O(N^2 \log N)$ operations (N: the dimension of the finest grid). In practice this results in algorithms for the solution of these integral equations that are significantly more efficient than the other schemes. In the present paper we apply multigrid methods to the following problems from fluid dynamics.

Calculation of potential flow around bodies - The total velocity potential ϕ is assumed to be the superposition of the potential ϕ_∞, due to a uniform onset flow and a perturbation potential ϕ_d, due to a doublet distribution at the body surface. This approach leads to a Fredholm equation of the second kind for the unknown doublet distribution. We introduce a multigrid method which makes use of a sequence of grids, that are generated by dividing the body surface into an increasing number of smaller and smaller panels. On these

grids the doublet distribution is assumed to be constant over each panel. For a two-dimensional (2-D) aerofoil we have applied the multigrid method to the calculation of circulatory flow around Kármán-Trefftz aerofoils. The use of multigrid techniques becomes more preferable for 3-D problems because the number of panels is much larger than for 2-D ones. The calculations have been performed for the flow around an ellipsoid. From numerical investigations it follows that ± 3 multigrid cycles are sufficient to obtain the approximate solution.

Calculation of oscillating disk flow - This application deals with the rotating flow due to an oscillating disk at an angular velocity $\Omega \sin \omega\tau$. The Navier-Stokes and continuity equations are reduced by means of the von Kármán similarity transformations to

$$\frac{\omega}{\Omega} f_t = \frac{\Omega}{2\omega} f_{zz} + 2hf_z - f^2 + g^2, \tag{2}$$

$$\frac{\omega}{\Omega} g_t = \frac{\Omega}{2\omega} g_{zz} + 2hg_z - 2fg, \tag{3}$$

$$h_z = f, \tag{4}$$

where (f,g,h) is a measure of the velocity vector in a cylindrical polar coordinate system (r,ϕ,z). For a single disk problem the boundary conditions are:

$$f = h = 0,\ g = \sin t \text{ at } z = 0;\ f = g = 0 \text{ for } z \to \infty. \tag{5}$$

In reference 3 the author has shown that the periodic solution:

$$h(z,0) = h(z,2\pi);\ g(z,0) = g(z,2\pi) \tag{6}$$

can be obtained by implicit finite difference schemes taking the state of rest as an initial condition. The transient effects have been eliminated by calculating a sufficiently large number of periods. Using the multigrid method we do not simulate the physical process, but reformulate the problem (2)-(6) as

$$(f,g,h) = K(f,g,h), \tag{7}$$

where K is a non-linear integral operator. The multigrid method for integral equations is used to solve (7). For $\Omega = 0.1\ \omega$ the computational work has been reduced by a factor 0.1.

The present paper is based on parts of the Doctor's Thesis of the author prepared under the guidance of Prof. P. Wesseling of Delft University of Technology.

CALCULATION OF POTENTIAL FLOW AROUND BODIES.

For potential flow around a two- or three-dimensional body there exists a velocity potential ϕ satisfying Laplace's equation

(8) $$\Delta \phi = 0$$

with boundary conditions,

(9) $$\frac{\partial \phi}{\partial n_e} = 0 \text{ along the boundary } S,$$

where $\frac{\partial}{\partial n_e}$ denotes differentiation in the direction of the outward normal to S and

(10) $$\phi(\zeta) \to \phi_\infty(\zeta) \quad \text{for } |\zeta| \to \infty ,$$

with ϕ_∞ the velocity potential due to a uniform onset flow. If the flow is non-circulatory, we have $\phi_\infty(\zeta) = U \cdot \zeta$, with U the velocity vector of the undisturbed flow. Here $U \cdot \zeta$ denotes the usual innerproduct in $\mathbb{R}^2$ or in $\mathbb{R}^3$. We represent the velocity potential ϕ as follows

$$\phi(\zeta) = \phi_\infty(\zeta) + \phi_d(\zeta),$$

with ϕ_d the double layer potential given by

(11) $$\phi_d(\zeta) = \frac{2^{1-m}}{\pi} \int_S \mu(z) \frac{\cos(n_z, z-\zeta)}{|z-\zeta|^{m-1}} dS_z , \quad \zeta \notin S ,$$

where m = 2,3 for the two- and three-dimensional case, respectively and n_z the outward normal to the boundary S at the point z. The doublet distribution μ is such that ϕ satisfies the boundary condition

(12) $$\phi^-(\zeta) = 0,$$

where ϕ^- denotes the limit from the inner side to S. Using the Plemelj-Privalov formulae (see reference 4) we obtain the following integral equation

$$(13) \qquad \mu(\zeta) + \frac{2^{2-m}}{\pi} \int_S \mu(z) \frac{\cos(n_z, z-\zeta)}{|z-\zeta|^{m-1}} dS_z = -2\phi_\infty(\zeta) , \qquad \zeta \in S.$$

Assuming the boundary S to be sufficiently smooth it can be proven that the solution of the interior Dirichlet-problem (12) also satisfies the Neumann-problem (8)-(10) for the exterior of the boundary S.

Calculation of Circulatory Flow around an Aerofoil.

For circulatory flow around an aerofoil one must introduce a cut to make the velocity potential single valued. The Kutta condition of smooth flow at the trailing edge can be satisfied if we construct the cut from the trailing edge to infinity.

We denote the upper and lower side of the cut by S^+ and S^-, respectively. The contour composed of the aerofoil S and the cut is denoted by $S^- + S + S^+$. Along the cut there exists a constant discontinuity in velocity potential. The jump is represented by a constant double layer potential with strength μ^+ and μ^- along S^+ and S^-, respectively. The difference $\mu^- - \mu^+$ is equal to the circulation which is taken positive in clockwise direction.

We can represent the velocity potential by

$$\phi(\zeta) = U \cdot \zeta + \frac{1}{2\pi} \int_{S^-+S+S^+} \mu(z) \frac{\cos(n_z, z-\zeta)}{|z-\zeta|} dS_z$$

or rewritten

$$(14) \qquad \phi(\zeta) = U \cdot \zeta + \phi_d(\zeta) + \frac{1}{2\pi} (\mu^+ - \mu^-) \arg(z_t - \zeta) ,$$

where ϕ_d is defined by (11) with m = 2 and z_t is the trailing edge. In this section we denote by $\arg(z_1/z_2)$ with $z_1, z_2 \in \mathbb{R}^2$ the real value of the usual function defined by the complex numbers corresponding to z_1 and z_2. The doublet strength along S follows from (12). So far we did not say anything about μ^+ and μ^-, but we still have to satisfy the Kutta condition. In the present paper we only consider aerofoils with non-zero trailing edge angle. For these cases the Kutta condition states that the flow speed must be zero at both sides of the trailing edge. Let ζ^+ and ζ^- be points at the upper and lower part of the trailing edge. The Kutta condition is satisfied if:

$$(15) \qquad \begin{cases} D\mu(\zeta^+) \to 0 & \text{for } |\zeta^+ - z_t| \to 0, \\ D\mu(\zeta^-) \to 0 & \text{for } |\zeta^- - z_t| \to 0, \end{cases}$$

where D denotes differentiation in the tangential direction. Application of conditions (12) and (15) to (14) yields the following integral equation

$$(16) \qquad (I-K)\mu + \beta(\mu^+ - \mu^-) = g,$$

with

$$(17) \qquad K\mu(\zeta) = \frac{-1}{\pi} \int_S \mu(z) \frac{\cos(n_z, z-\zeta)}{|z-\zeta|} dS_z ,$$

$$\beta(\zeta) = \frac{1}{\pi} \arg(z_t - \zeta) ,$$

$$g(\zeta) = -2\, U \cdot \zeta .$$

Numerical approach - The contour S is divided into N segments S_i such that $S = \bigcup_{i=1}^{N} S_i$ and $S_i \cap S_j = \emptyset$, $i \neq j$. The begin- and end-points of the i^{th} segment are z_{i-1} and z_i and are called nodal points. On this grid μ is approximated by a piecewise constant function μ_N and the resulting equation is solved by a collocation method. The collocation points ζ_i, i = 1,2,..., N, are taken to be the mid-points of the segments S_i. By means of projection at the collocation points we get N equations. However, we have N + 2 unknowns $\mu_{N,1}, \mu_{N,2}, \ldots, \mu_{N,N}, \mu_N^+$ and μ_N^- with $\mu_{N,i} = \mu_N(\zeta_i)$ and $\mu_N^{\pm} = \mu_N(\zeta; \zeta \in S^{\pm})$, so that we need two extra equations. Following condition (15) we replace μ_N^+ and μ_N^- by $\mu_{N,N}$ and $\mu_{N,1}$, i.e.

$$(18) \qquad \begin{cases} \mu_N^+ = \mu_N(\zeta_N), \\ \mu_N^- = \mu_N(\zeta_1), \end{cases}$$

where ζ_1 and ζ_N are the collocation points which are closest to the trailing edge at the lower and upper part of S. Let T_N be the projection operator defined by piecewise constant interpolation at the collocation points. We have to solve the following equation

$$(19) \qquad (I-T_N K)\mu_N + T_N \beta (\mu_{N,N}-\mu_{N,1}) = T_N g.$$

In aerodynamics the above numerical approach is called a first order panel method. In reference 5 we have put it in a functional analytic framework. Assuming the contour S to be sufficiently smooth (except for a small region near the trailing edge) it was shown that a once continuously differentiable numerical solution can be obtained by a single iteration

$$(20) \qquad \tilde{\mu}_N = g + (\mu_{N,N} - \mu_{N,1})\beta + K\mu_N \ .$$

Furthermore, it was proven that the operator K is compact on the space of essentially bounded functions, provided the boundary is sufficiently smooth. Since aerofoils (inclusive the trailing edge) are not smooth this property of K does not hold for our application.

Multigrid method - The principal aim of this section is to show that equation (19) can be solved efficiently by a multigrid iterative process. In reference 2 we introduced multigrid methods for integral equation (1). The Jacobi-relaxation was used to smooth the high-frequency errors. Assuming the integral operator to be compact we were able to prove that the reduction factors of these multigrid methods decrease as N increases. For our application this nice property is completely destroyed (see table 1) because K is not compact. Problems with respect to the convergence of the iterative process arise in the neighbourhood of the trailing edge. Here the high-frequency errors are not removed by the Jacobi-relaxation:

$$(21) \qquad \mu_N^{(\nu+1)} = T_N g + T_N K \mu_N^{(\nu)} - T_N \beta(\mu_{N,N}^{(\nu)} - \mu_{N,1}^{(\nu)}).$$

Inspection of the matrix corresponding to $T_N K T_N$ reveals that the cross-diagonal contains elements of magnitude $k-1 + O(1/N)$ as $N \to \infty$ with k = (exterior trailing edge angle $)/\pi$. This occurrence of off-diagonal elements of about the same size as diagonal elements explains why Jacobi-relaxation does not work well. Therefore we apply another relaxation scheme, which we call *paired Gauss-Seidel relaxation*. In order to explain this scheme we first rewrite (21) as follows:

$$\mu_{N,i}^{(\nu+1)} = g_i + \sum_{\ell=1}^{N} k_{i\ell} \mu_{N,\ell}^{(\nu)} - \beta_i(\mu_{N,N}^{(\nu)} - \mu_{N,1}^{(\nu)}) \text{ for } i = 1(1)\,N.$$

We obtain the *paired Jacobi relaxation* (PJ) scheme by removing the cross-diagonal to the left-hand side:

$$\mu_{N,i}^{(\nu+1)} - k_{ij} \mu_{N,j}^{(\nu+1)} = g_i + \sum_{\substack{\ell=1 \\ \ell \neq j}}^{N} k_{i\ell} \mu_{N,\ell}^{(\nu)} - \beta_i(\mu_{N,N}^{(\nu)} - \mu_{N,1}^{(\nu)}),$$

for $i = 1,2,\ldots, N/2$ and $j = N+1-i$. A similar expression is obtained for $i = j$. As a result we have to solve $\frac{1}{2}N$ systems of equations of dimension 2. Substituting the new values of $\mu_{N,i}$ and $\mu_{N,j}$ as soon as they are available we obtain the paired Gauss-Seidel (PGS) relaxation scheme. For $i = 1,2,\ldots, N/2$ and $j = N+1-i$ we define

$$\nu_{\ell i} = \begin{cases} \nu & \text{for } i \leq \ell \leq j, \\ \nu+1 & \text{for } \ell < i \text{ and } \ell > j. \end{cases}$$

We solve simultaneously the following equations

$$\mu_{N,i}^{(\nu+1)} - k_{ij} \mu_{N,j}^{(\nu+1)} = g_i + \sum_{\substack{\ell=1 \\ \ell \neq j}}^{N} k_{i\ell} \mu_{N,\ell}^{(\nu_{\ell i})} - \beta_i(\mu_{N,N}^{(\bar{\nu})} - \mu_{N,1}^{(\bar{\nu})})$$

and

$$\mu_{N,j}^{(\nu+1)} - k_{ji} \mu_{N,i}^{(\nu+1)} = g_j + \sum_{\substack{\ell=1 \\ \ell \neq i}}^{N} k_{j\ell} \mu_{N,\ell}^{(\nu_{\ell i})} - \beta_j(\mu_{N,N}^{(\bar{\nu})} - \mu_{N,1}^{(\bar{\nu})}),$$

for $i = 1,2,\ldots, N/2$ and $j = N+1-i$, with $\bar{\nu} = \nu$ for $i = 1$ and $\bar{\nu} = \nu + 1$ for $1 < i \leq N/2$. The matrix elements k_{ij} can be easily calculated. Let

$$\phi_{ij} = \frac{1}{\pi} \arg \frac{z_j - \zeta_i}{z_{j-1} - \zeta_i} ,$$

then

$$k_{ij} = \begin{cases} \phi_{ij} & \text{for } i \neq j , \\ \phi_{ii} + \begin{cases} 1 & \text{if } \phi_{ii} < 0 , \\ -1 & \text{if } \phi_{ii} > 0 . \end{cases} \end{cases}$$

Let X_p be a short notation for the space X_{N_p} of piecewise constant functions of dimension N_p. We introduce a sequence of spaces $\{X_p \mid p = 0,1,\ldots, \ell\}$ with $N_p = 32 * 2^p$ such that

$$X_0 \subset X_1 \subset \ldots \subset X_\ell .$$

The corresponding projection operators are denoted by T_p. In the context of multigrid iteration the subscript p is called level.

The calculations have been performed for several Kármán-Trefftz aerofoils with thickness $\delta = 0.05$ and length $\ell = 1.0$. These aerofoils are obtained from the circle in the x-plane, $x = c\, e^{i\theta}$, by means of the mapping

$$z = f(x) = (x - x_t)^k / (x - c(\delta - i\gamma))^{k-1},$$

where γ measures the camber and k the exterior trailing edge angle;

$$c = 2\ell \left(\delta + (1-\gamma^2)^{\frac{1}{2}}\right)^{k-1} / \left(2(1-\gamma^2)^{\frac{1}{2}}\right)^k ,$$

$$x_t = c\left((1-\gamma^2)^{\frac{1}{2}} - i\gamma\right).$$

Partition of the boundary on level p: Let the interval $[0,2\pi]$ be divided into N_p uniform segments with nodal points $\{\theta_j \mid j = 0(1)N_p\}$. The nodal- and collocation-points in the z- plane follow from $f(ce^{i\theta_j})$ and $f(ce^{i\theta_{j+\frac{1}{2}}})$, respectively, $\theta_{j+\frac{1}{2}}$ being the midpoint of subinterval $[\theta_j, \theta_{j+1}]$. The collocation points defined in this way are situated at the boundary and do not coincide

with the collocation points of the other levels. Therefore, the elements of the matrix K_p , p = 0,1,..., ℓ, corresponding to $T_p K T_p$ have to be computed for all levels. Asymptotically for $\ell \to \infty$, the number of kernel evaluations is $\frac{4}{3} N_\ell^2$, when the values are computed once and stored. We have taken the following testcases:

I. k = 1.90 and γ = 0,

II. k = 1.90 and γ = sin 0.05,

III. k = 1.99 and γ = 0,

IV. k = 1.99 and γ = sin 0.05.

The velocity U of the undisturbed flow is taken to be (cos τ, sin τ) with τ the angle of incidence. For the above testcases we give numerical results for τ = 0 and $\tau = \pi/2$.

Algorithm: The approximate solution of (19) is obtained by the multigrid method defined in the ALGOL-68 program given in TEXT 1:

```
PROC mulgrid = (INT p,σ, VEC u,g) VOID:
IF p = 0
THEN solve directly (u,g)
ELSE  FOR  i TO σ
      DO   relax (u,g); INT n = UPB u ;
           VEC residu = g-u+K_p*u-β_p*(u[n] - u [1]);
           VEC um := 0_(p-1), gm := restrict (residu);
           mulgrid (p-1, ν,  um, gm );
           u := u + interpolate (um);
           relax (u,g)
      OD
FI
```

TEXT 1. Multigrid algorithm.

Because of reasons of efficiency the number of coarse grid corrections (integer ν) must be less than 4. For ν = 1 and ν = 2 we obtain the so-called V- and W-cycle, respectively. Here we choose ν = 2. For the 3-D problem of flow around an ellipsoid we take ν = 1. The interaction between the grids is

defined by the procedures *restrict* and *interpolate* which are specified as follows. Let n be the upper bound of *VEC u*, then:

*restrict (u) [i] := 0.5 * (u [2*i-1] + u[2*i]), i = 1(1)n/2,*

*interpolate (u)[2*i] := interpolate (u) [2*i-1] := u [i], i = 1(1)n.*

On level 0 the system of equations is solved by Gaussian elimination. For *relax* we take: Jacobi -, paired Jacobi - and paired Gauss-Seidel relaxation, respectively. We start our algorithm on level 0. The interpolation to level p ($p \geq 1$) of the approximate solution from level p-1 is used as initial guess of the multigrid process at level p; truncation occurs when the residual is less than 10^{-6}. Let *VEC* g_p denote the restriction of g to the collocation points of level p. In ALGOL-68 notation this algorithm reads:

```
solve directly (u0,g0);
FOR p TO 3
DO    up := interpolate (u0);
      FOR i TO 25 WHILE residual > 10^-6
      DO mulgrid (p, 1, up, gp) OD;
      u0 := COPY up
OD;
```

TEXT 2. Implementation of the full multi-grid algorithm.

In the following table we compare the performance of the multigrid processes using various relaxation schemes.
From this table we conclude that the multigrid method defined by Jacobi-relaxation is <u>not</u> acceptable (it converges too slowly). The process defined by PGS-relaxation turns out to be the most efficient. Furthermore, we draw the following conclusions: 1. the number of iterations decreases as N increases and 2. on the highest level (N=256) only a few iterations are necessary.

TABLE 1 - NUMBER OF ITERATIONS

Testcase	τ	N = 64			N = 128			N = 256		
		J	PJ	PGS	J	PJ	PGS	J	PJ	PGS
I	0	15	4	3	13	3	2	11	3	2
	π/2	15	9	9	4	7	5	2	4	2
II	0	15	8	8	13	5	5	11	3	2
	π/2	15	10	9	9	7	6	6	4	2
III	0	>25	4	3	>25	3	3	>25	3	2
	π/2	> 25	12	9	19	9	6	9	6	3
IV	0	> 25	11	8	>25	7	4	>25	6	4
	π/2	> 25	13	10	>25	10	8	>25	7	3

J - Jacobi , PJ - Paired Jacobi, PGS - Paired Gauss-Seidel.

Calculation of Potential Flow around an Ellipsoid.

The numerical approach to find the solution of (13) is connected with the shape of the kernel-function. Application of the collocation method in the space of piecewise constant functions leads to moment-integrals, which consist of the calculation of solid angles. We consider the ellipsoid defined by

$$\frac{x}{4}^2 + y^2 + z^2 = 1 .$$

The velocity of the undisturbed flow is given by $U = (1,0,0)$. The partition of the ellipsoid into panels is carried out as follows. First we divide the surface into N rings by planes orthogonal to the z-axis. Next each ring is divided into N^* trapeziform segments. The spherical caps are divided into N^* triangle-form segments. We denote these segments by S_{ij} , $i = 1(1)N$ and $j = 1(1)N^*$. The collocation points are chosen to be the "midpoints" of these segments and are situated at the surface. The solid angle subtended at ζ by S_{ij} with $\zeta \notin S_{ij}$ is given by

$$\int_{S_{ij}} \frac{\cos(n_z, z-\zeta)}{|z-\zeta|^2}\, dS_z \ .$$

In contrast with 2-D in general these integrals cannot be evaluated analytically. We approximate S_{ij} by one or two flat planes. The solid angles subtended by such planes can be evaluated analytically.

Multigrid method - The different grids are related by $N_p = 4 * 2^p$ and $N_p^* = 4 * 2^p$. Putting $\beta_p = 0$ we use the algorithm given in TEXT 1 with $\nu = 1$. Analogously to 2-D we define the procedures *solve directly*, *restrict* and *interpolate* by Gaussian elimination, weighted injection and piecewise constant interpolation, respectively. For *relax* we take the Jacobi-relaxation scheme. Assuming the surface to be smooth Wolff (ref.6) has analysed this multigrid method. He has proven that the reduction-factor of the multigrid process is less than ch^{α} for $h \to 0$, where h and α are a measure for the mesh-size and the smoothness of the surface, respectively. For the ellipsoid $\alpha = 1$.

Numerical results - In table 2 we give the residuals and the observed reduction factors

$$\eta_i = \| \mu_N^{(i+1)} - \mu_N^{(i)} \| / \| \mu_N^{(i)} - \mu_N^{(i-1)} \| ,$$

with $\| \ . \|$ the supremum norm. We also give the mean reduction factor

$$\bar{\eta} = \{ \prod_{i=1}^{k} \eta_i \}^{1/k}$$

and the operation count expressed in work-units. One work-unit is defined by (total number of multiplications)/$(N_\ell * N_\ell^*)^2$ with ℓ the highest level. We only take into account matrix-vector multiplications and the direct solution on the coarsest grid for which we count $\frac{1}{3}(N_0 * N_0^*)^3$ multiplications. Table 2 enables us to draw the following conclusions: 1. Comparing the results obtained with $\ell = 2$ and $\ell = 3$ we see that the mean reduction factor of the multigrid

TABLE 2 - POTENTIAL FLOW AROUND AN ELLIPSOID *

MULTIGRID METHOD ($N_0 = 4$, $N_0^* = 4$)								
$\ell = 2$; $N_2 = 16$, $N_2^* = 16$					$\ell = 3$; $N_3 = 32$, $N_3^* = 32$				
iter	residual		red. factor		iter	residual		red. factor	
1	$1.17\ 10^{-1}$				1	$4.56\ 10^{-2}$			
2	$2.04\ 10^{-3}$		$4.13\ 10^{-2}$		2	$4.38\ 10^{-4}$		$1.67\ 10^{-2}$	
3	$7.75\ 10^{-5}$		$1.40\ 10^{-2}$		3	$8.48\ 10^{-6}$		$6.98\ 10^{-3}$	
4	$1.89\ 10^{-6}$		$4.63\ 10^{-2}$		4	$9.93\ 10^{-8}$		$2.56\ 10^{-2}$	
5	$6.54\ 10^{-8}$		$2.36\ 10^{-2}$						
mean red. factor: $2.83\ 10^{-2}$					mean red. factor: $1.44\ 10^{-2}$				
operation count : 10.68					operation count : 8.53				
JACOBI ITERATIVE PROCESS									
$N = 16$, $N^* = 16$					$N = 32$, $N^* = 32$				
iter	residual		red. factor		iter	residual		red. factor	
1	1.73				1	2.15			
2	$8.05\ 10^{-1}$		$4.51\ 10^{-1}$		2	1.20		$5.44\ 10^{-1}$	
3	$3.82\ 10^{-1}$		$4.68\ 10^{-1}$		3	$6.72\ 10^{-1}$		$5.57\ 10^{-1}$	
4	$1.83\ 10^{-1}$		$4.75\ 10^{-1}$		4	$3.79\ 10^{-1}$		$5.62\ 10^{-1}$	
5	$8.75\ 10^{-2}$		$4.78\ 10^{-1}$		5	$2.14\ 10^{-1}$		$5.64\ 10^{-1}$	
6	$4.20\ 10^{-2}$		$4.79\ 10^{-1}$		6	$1.21\ 10^{-1}$		$5.65\ 10^{-1}$	
7	$2.01\ 10^{-2}$		$4.80\ 10^{-1}$		7	$6.85\ 10^{-2}$		$5.65\ 10^{-1}$	
⋮	⋮		⋮		8	$3.88\ 10^{-2}$		$5.66\ 10^{-1}$	
					⋮	⋮		⋮	
21	$6.94\ 10^{-7}$		$4.80\ 10^{-1}$		27	$7.79\ 10^{-7}$		$5.66\ 10^{-1}$	
mean red. factor: $4.77\ 10^{-1}$					mean. red. factor: $5.64\ 10^{-1}$				
operation count : 21					operation count : 27				

* $\frac{x}{4} + y^2 + z^2 = 1$, U parallel to the x - axis.

method has been decreased by a factor 2, which is in agreement with the theoretical results of Wolff (ref.6) and 2. the multigrid method is much cheaper than the Jacobi-iterative process.

CALCULATION OF OSCILLATING DISK FLOW.

The rotating flow due to an infinite disk performing torsional oscillations at an angular velocity $\Omega \sin \omega\tau$ in a viscous fluid otherwise at rest involves two relevant length scales : 1. the Von Kármán layer thickness $(\nu/\Omega)^{1/2}$, where ν is the kinematic viscosity and 2. the Stokes layer thickness $(\nu/\omega)^{1/2}$. By means of the Von Kármán similarity transformations the velocities (u,v,w) in a cylindrical coordinate system (r,ϕ,x) can be written as:

$$u = \Omega r f(z,t) \ , \ v = \Omega r g(z,t) \ , w = - 2(2\nu\omega)^{1/2} \ h(z,t),$$

where $z = (\frac{\Omega^2}{2\nu\omega})^{1/2} x$ and $t = \omega\tau$. In that case the Navier-Stokes equations reduce to the partial differential equations (2) - (4). Apparently the oscillating disk flow is characterized by the parameter $\varepsilon = \Omega/\omega$, which determines the ratio of the Stokes layer thickness to the Von Kármán layer thickness.

For the high-frequency flow ($\varepsilon << 1$) analytical solutions are found in the literature in the form of series expansions in terms of ε. This type of flow consists of an oscillatory inner layer (i.e. Stokes layer) near the rotating disk and a secondary outer layer (i.e. Von Kármán layer). Using a multiple scaling technique Benney (ref.7) was able to find series expansions valid throughout the region of flow. The first order terms of the solution are given by:

$$(22) \qquad g(z,t) = e^{-z/\varepsilon} \sin(t-z/\varepsilon) \ , \ f(z,t) \sim \varepsilon \, e^{-4az} \text{ for } z \to \infty \ ,$$

with a = 0.265. In reference 3 we used this technique to determine the axial inflow at infinity up to the term with ε^3 :

$$h(\infty,0) = a\varepsilon + \{ab + \frac{1}{16}(\sqrt{2}-1)\}\varepsilon^2 + O(\varepsilon^3), \tag{23}$$

with b = - 0.207 . Inspection of (22) reveals that problem (2) - (6) is singularly perturbed and for a fixed t the solution contains more and more high frequency components as $\varepsilon \to 0$.

In this paper we discuss two computational methods to find the periodic solution satisfying (6). The first method is based on simulation of the physical process by taking the state of rest as an initial condition and eliminating the transient effects by integration in time. In mathematical terminology this process can be interpreted as Picard's method for computing a fixed point. Let the velocity vector be:

$$v = (f,g,h).$$

Denote by $(v(z,t); v_0)$ the solution of the usual initial-value problem (2)-(5) with initial data:

$$v(z,0) = v_0(z). \tag{24}$$

Assume that the initial data v_0 belong to a suitable class L. Define a map of L into itself by the equation

$$K_\varepsilon(v_0) := (v(\cdot,2\pi); v_0) , \tag{25}$$

being the solution of (2) - (5) and (24) at $t = 2\pi$. Since (2)-(4) is a parabolic system K_ε may be expected to have a smoothing influence, just as the integral operators of the Fredholm equations studied in reference 2. In operator notation simulation of the physical process is written as the Picard sequence

$$v_{i+1} = K_\varepsilon(v_i) \text{ with } v_0 = 0. \tag{26}$$

The periodic condition (6) rewrites as

(27) $$v = K_\varepsilon(v), \quad v \in L.$$

We remark that K_ε is a non-linear operator. For $\varepsilon < 1$ (26) converges slowly. Therefore we have devised another method. Since equation (27) has a superficial resemblance with a Fredholm equation of the second kind we have applied a multigrid method to (27).

Numerical Approach

This section is divided into two parts: 1. the numerical solution of the initial-boundary value problem (2) - (5) with the initial data (24) and 2. numerical methods for finding periodic solutions satisfying (6).

Discretization of the initial-boundary value problem - Consider the partial differential equations (2) -(4) with the boundary conditions (5) and the initial data (24). To this problem we apply implicit finite difference techniques in combination with an appropriate stretching function for the construction of the computational grid. In calculations the boundary conditions at infinity are applied at a finite value $z = \ell$:

(28) $$f(\ell,t) = g(\ell,t) = 0.$$

We want to resolve the flow structure near the disk with a limited number of mesh points. Therefore, taking into account (22) we transform the z-coordinate by:

(29) $$z(x) = \ell(\varepsilon x + (1-\varepsilon)x^3) \ , \quad x \in [0,1],$$

and we take the mesh covering of the new range $0 \le x \le 1$ uniform with stepsize $\Delta x = {}^1/N$. Integration in time is done by the Euler-backward formula:

$$g_t = \frac{g_{k+1} - g_k}{\Delta t} \quad \text{,with } \Delta t = 2\pi/T \ .$$

The right-hand sides of (2) - (3) are discretized by central differences at $t = t_{k+1}$. The left- and right- hand side of (4) are integrated by means of the mid-point and trapezoidal rule, respectively. The resulting non-linear system of finite difference equations is solved by means of Newton iteration,

which is terminated if the residual is less than 10^{-6}. For further details see reference 3.

Numerical methods for computing periodic solutions - Using the above finite difference approach we define the discrete counterpart of the operator K_ε and the velocity vector v by $K_{\varepsilon;\,N,T,\ell}$ and v_N respectively. In discrete operator notation the periodic condition reads:

$$v_N = K_{\varepsilon;\,N,T,\ell}\,(v_N). \tag{30}$$

In the present paper we propose two computational methods to solve (30) : A. simulation of the physical process by Picard iteration and B. a multigrid method. In the first method the parameters ε, N, T and ℓ are fixed. In the second method the parameters N and T are taken from a sequence $\{(N_p,T_p)\}$, $p = 0,1,\ldots, L$ such that with $p = L$ we have $N_L = N$, $T_L = T$ and with $p < q \le L$ we have $N_p \le N_q$, $T_p \le T_q$ (i.e. a smaller p corresponds with a coarser discretization).

A. Simulation of the physical process: We take the state of rest ($v_N^{(0)} \equiv 0$) as an initial condition. The transient effects are eliminated by Picard's method:

$$v_N^{(i+1)} = K_{\varepsilon;N,T,\ell}\,(v_N^{(i)}). \tag{31}$$

The iteration index i counts the number of periods that is calculated. This process is truncated if the residual $\| v_N^{(i)} - K_{\varepsilon;N,T,\ell}\,(v_N^{(i)})\|$ is less than $0.5\ \ 10^{-4}$. Here

$$\|v_N\| = \max_{0\le j\le N} |\,g_j\,| + \max_{0\le j\le N} |\,h_j\,| .$$

B. Multigrid method: We introduce a sequence of grids with $N_p = 20 * 2^p$ and $T_p = 8 * 2^p$. The integer p is called level. We replace the subscript N_p by p:

$$v_{N_p} = v_p \text{ and } K_{\varepsilon;\,N_p,\,T_p,\ell} = K_{\varepsilon;\,p}\,.$$

Denote the velocity at grid point x_j on level p by $v_p[j] = (f_j,g_j,h_j)$. The

addition v_p [j] + v_p [k] and the multiplication c * v_p [j] are defined as usual (element by element). The interaction between the grids is defined by piecewise-linear interpolation:

$$\textit{interpolate}\ (U)\ [j] = \begin{cases} U[j/2], & j = 0,2,\ldots, 2N, \\ 0.5 * (U[\frac{j+1}{2}] + U[\frac{j-1}{2}]), & j = 1,3,\ldots, 2N-1, \end{cases}$$

and by injection:

$$\textit{restrict}\quad (U)\ [j] = U\ [2j]\ ,\ j = 0,1,\ldots, \frac{N}{2}\ ,$$

where N is the upper-bound of the velocity vector U.

We use a multigrid method that starts on level 0 with simulation of the physical process (method A). For small values of ε we apply continuation. Suppose we have the following ε-sequence $\{\varepsilon_\ell \mid \varepsilon_0 > \varepsilon_1 > \ldots > \varepsilon_m$ with $\varepsilon_0 = 1\}$. At each stage of this continuation process we approximately solve the equation $v_0 = K_{\varepsilon_\ell\ ;\ 0}\ (v_0)$ by (31) until the residual is less than $0.5\ 10^{-3}$. As initial guess of (31) we take the solution of the previous stage ($\varepsilon=\varepsilon_{\ell-1}$). For $\varepsilon = \varepsilon_0$ we take the state of rest. Denote the solution of this continuation method by $v_0\ (\varepsilon_0,\varepsilon_1,\ldots,\varepsilon_m)$.

Since (30) is a non-linear equation it is only solved approximately. Let U_p be an approximation to the solution v_p of (30) on level p. We define the defect of U_p by

$$d_p = U_p - K_{\varepsilon;p}\ (U_p)\ .$$

The multigrid method is given by the ALGOL -68 program in TEXT 3, where *VELO* is a mode for the vector of unknowns:

```
MODE VELO = STRUCT (VEC f,g, h) .

PROC compute periodic solution = ( # to level # INT ℓ) VOID:
(U0 := v0(ε0,ε1,...,εm);
 FOR j TO ℓ
 DO   dj-1 := Uj-1 - Kε; j-1 (Uj-1) ;
      Uj := interpolate (Uj-1);
      multigrid (j,1,Uj,0j)
 OD
 );
```

```
PROC multigrid = (INT m, σ, REF VELO U, VELO y) VOID:
(IF m = 0
 THEN FOR k TO 50 WHILE residual > δ_ε
      DO VELO r = y - U + K_ε;m (U);
         residual := ‖r‖;
         U := U + ω_k * r
      OD
 ELSE FOR i TO σ
      DO  U := y + K_ε;m (U);
          VELO d = d_m-1-restrict (y-U + K_ε;m(U));
          VELO v :=  COPY U_m-1;
          multigrid (m-1, 2, v, d);
          U := U + interpolate (U_m-1 - v)
      OD
 FI
);
```

TEXT 3 Multigrid algorithm for the computation of periodic solutions of parabolic equations.

The structure of this multigrid algorithm has been proposed by Hackbusch (ref.8) for the numerical solution of general time-periodic parabolic problems. Here we apply it to the particular problem of oscillating disk flow.

On level 0 of *multigrid* we use overrelaxation for extremely small values of ε. The parameter ω_k takes the values 1,2 and 4. Initially we put $\omega_k = 1$. If the axial inflow converges slowly it is multiplied by a factor 2. As soon as the residual increases the value $\omega_k = 1$ is restored.

Numerical results - From Zandbergen and Dijkstra (ref.9) it is known that Von Kármán's rotating disk solution can be represented sufficiently accurate with $\ell = 12$, hence we fix infinity at this value. We give numerical results for the following values of ε :

$$\varepsilon_0 = 1 \ , \ \varepsilon_1 = 0.5 \ , \ \varepsilon_2 = 0.1 \ , \ \varepsilon_3 = 0.05.$$

This sequence is also applied in the continuation process that is used to find an approximation U_0 of the multigrid method, e.g. for $\varepsilon = 0.1$ we have $U_0 := v_0\ (1, 0.5, 0.1)$. For N = 160 and T = 64 we compare the performance of simulation of the physical process (method A) and the multigrid method (B). On the coarsest grid the latter method needs 20 stepsizes in space and 8 stepsizes in time; hence it uses four levels: 0,1, 2 and 3.

Let a work unit be defined by the computational work needed for calculating one Picard iterate with N = 160 and T = 64. In table 3 we compare the computed axial inflow at infinity with the value of its asymptotic approximation (23) for $\varepsilon \to 0$. Between parentheses we give the number of work units and the iteration error $\| U_N - K_{\varepsilon;\, N,T,\, \ell}\,(U_N) \|$, where U_N is the final solution.

On level 0 of the multigrid method we used Picard iteration (i.e. $\omega_k \equiv 1$) for $\varepsilon \geq 0.1$. The iterative process was terminated when the residual was less than $\delta_\varepsilon = 0.5\ \ 10^{-4}$. For $\varepsilon = 0.05$ we have applied overrelaxation ($1 \leq \omega_k \leq 4$) and we have put $\delta_{0.05} = 10^{-7}$. That is the reason why the computational work increased for this case.

TABLE 3 AXIAL INFLOW*

ε	method A	method B	(23)
1.0	0.2014 (8, 4.4 10^{-5})	0.2014 (6.8, 9.3 10^{-7})	0.2360
0.5	0.1177 (17, 4.7 10^{-5})	0.1178 (7.0, 3.9 10^{-6})	0.1253
0.1	0.0236 (74, 4.9 10^{-5})	0.0271 (7.4, 1.6 10^{-5})	0.0262
0.05	0.0083 (72, 4.9 10^{-5})	0.0137 (12.5, 3.3 10^{-6})	0.0132

* Between parentheses : number of work units, residual.

From table 3 we conclude that the multigrid method becomes more efficient as ε decreases. For $\varepsilon = 0.1$ the computational work has been reduced by

a factor 1/10. For $\varepsilon = 0.1$ and $\varepsilon = 0.05$ the numerical results of method A still contain a low-frequency error. In this case the test for termination of the physical process is not adequate. The process converges slowly, as can be seen from figure 1, in which we have displayed the axial inflow as a function of the number of periods. For $\varepsilon = 0.05$ the axial inflow is still increasing after 72 periods. The same phenomenon occurs on the coarsest grid of the multigrid method. Therefore we have applied overrelaxation.

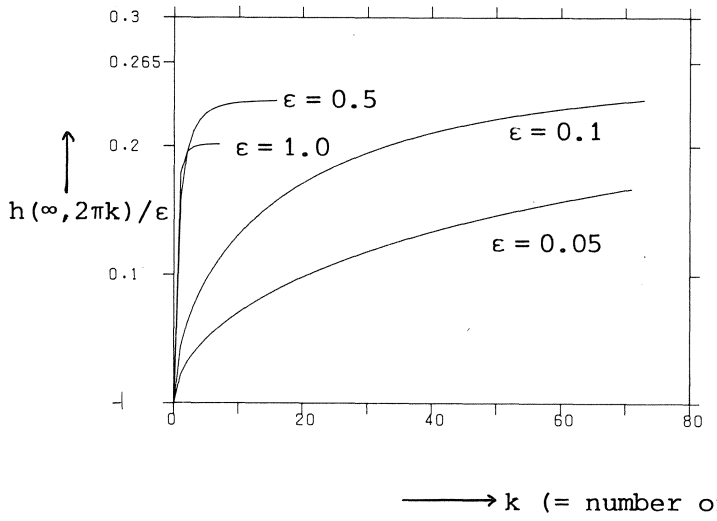

FIGURE 1. Dependence of the axial inflow on the number of periods

The results of our analysis are given in figures 2-3. The profiles of the variables f/ε , g and h/ε are displayed in figure 2. We see that there is an oscillatory boundary layer. For smaller values of ε (see figures 2 (c-d)) the azimuthal component of velocity (g) is confined to this boundary layer and the radial and axial component of velocity (resp. f and h) persist outside this layer. The results for the quantities $\varepsilon\, g_z(0,t)$, $f_z(0,t)$ and $h(\infty,t)/\varepsilon$ are displayed in figure 3. Comparing these figures we see that the fluctuations in $h(\infty,t)$ decrease as $\varepsilon \to 0$. This means that outside the boundary layer the fluid motion becomes stationary (i.e. the outer flow does not depend on t). These numerical results are in agreement with the analytical solutions of Benney (ref.7).

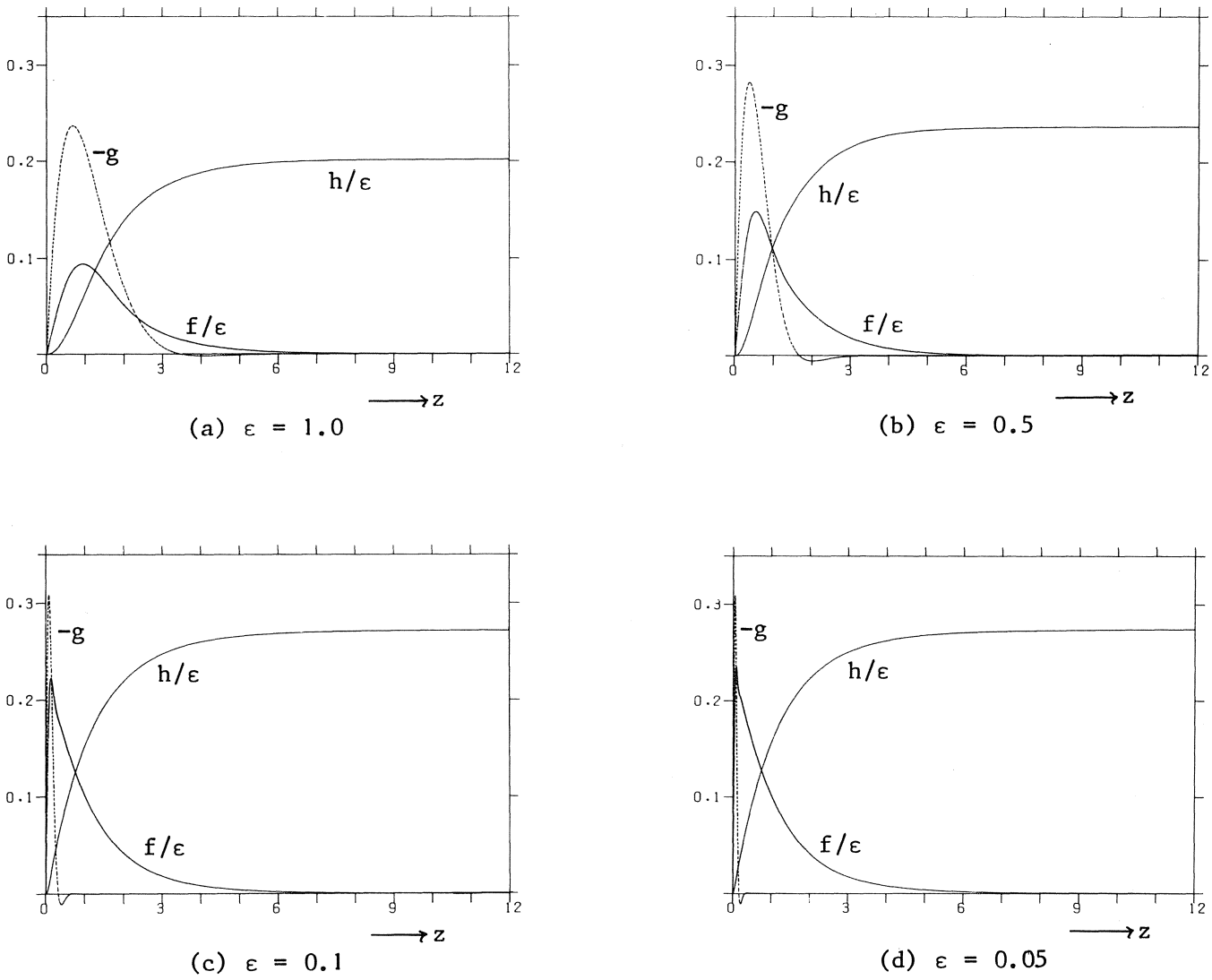

FIGURE 2. Velocity profiles

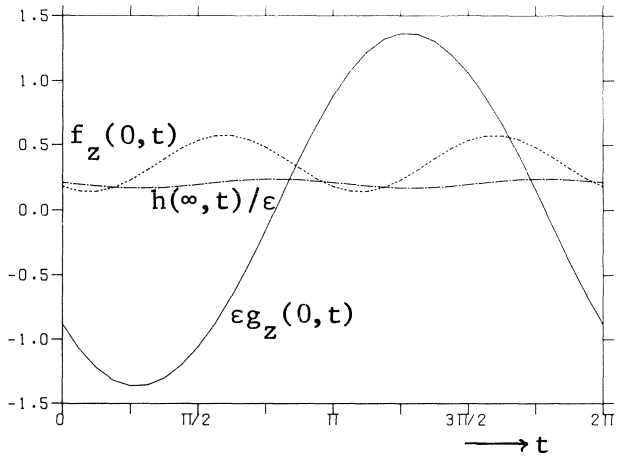

(a) $\varepsilon = 1.0$

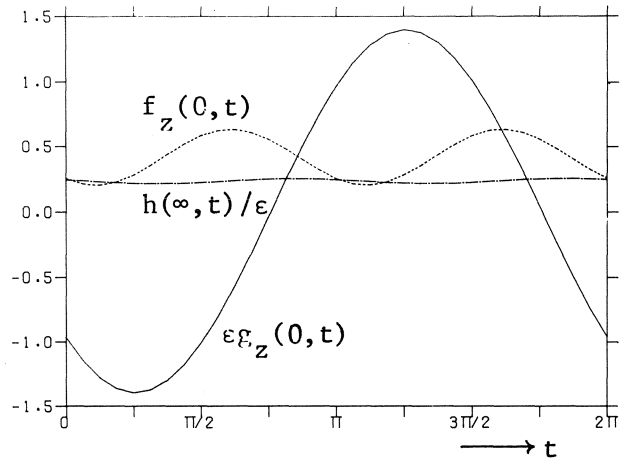

(b) $\varepsilon = 0.5$

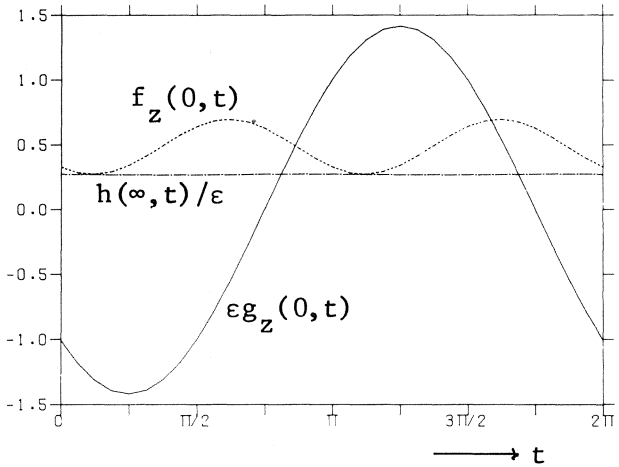

(c) $\varepsilon = 0.1$

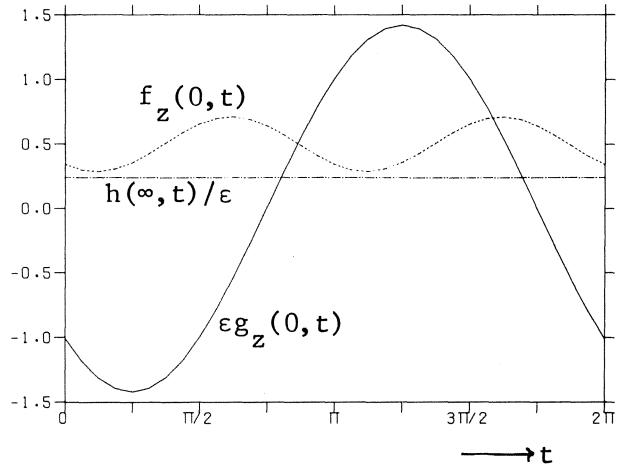

(d) $\varepsilon = 0.05$

FIGURE 3. Axial inflow and shear stresses

Finally, from the results just presented we conclude that for the computation of periodic solutions of the single disk problem for $\varepsilon \leq 1$ the multigrid method is preferable, whereas for $\varepsilon > 1$ simulation of the physical process may be employed.

REFERENCES

[1] BRANDT, A., *Multi-level adaptive solutions to boundary-value problems*, Math. Comp., vol. 31, no. 138, Apr. 1977, pp. 333-390.

[2] HEMKER, P.W. & H. SCHIPPERS, *Multiple grid methods for the solution of Fredholm integral equations of the second kind*, Math. Comp., vol. 36, no. 153, Jan. 1981, pp. 215-232.

[3] SCHIPPERS, H., *Analytical and numerical results for the nonstationary rotating disk flow*, J. Engng. Math., vol. 13, no. 2, Apr. 1979, pp. 173-191.

[4] MUSCHELISCHWILI, N.I., *Singuläre Integralgleichungen*, Akademie-Verlag, Berlin, 1965.

[5] SCHIPPERS, H., *On the regularity of the principal value of the double layer potential*, to be published in J. Engng. Math.

[6] WOLFF, H., *Multigrid method for the calculation of potential flow around 3-D bodies*, Master's thesis University of Amsterdam, to appear as MC report NW, Mathematisch Centrum, Amsterdam, 1981.

[7] BENNEY, D.J., *The flow induced by a disk oscillating in its own plane*, J. Fluid Mech., vol. 18, no. 3, March 1964, pp. 385-391.

[8] HACKBUSCH, W., *The fast numerical solution of time-periodic problems*, Report 79-14, Mathematisch Institut, Universität zu Köln, 1979.

[9] ZANDBERGEN, P.J. & D. DIJKSTRA, *Non-unique solutions of the Navier-Stokes equations for the Kármán swirling flow*, J. Engng. Math., vol. 11, no. 2, April 1977, pp. 167-188.